

## SHORT COMMUNICATION

# The fermentation product 2,3-butanediol alters *P. aeruginosa* clearance, cytokine response and the lung microbiome

Mytien Nguyen<sup>1,4</sup>, Anurag Sharma<sup>2,4</sup>, Wenzhu Wu<sup>3</sup>, Rika Gomi<sup>2</sup>, Biin Sung<sup>3</sup>,  
Denina Hospodsky<sup>1</sup>, Largus T Angenent<sup>1,4</sup> and Stefan Worgall<sup>2,3,4</sup>

<sup>1</sup>Department of Biological and Environmental Engineering, Cornell University, Ithaca, NY, USA;

<sup>2</sup>Department of Pediatrics, Weill Cornell Medicine, New York, USA and <sup>3</sup>Department of Genetic Medicine, Weill Cornell Medicine, New York, USA

Diseases that favor colonization of the respiratory tract with *Pseudomonas aeruginosa* are characterized by an altered airway microbiome. Virulence of *P. aeruginosa* respiratory tract infection is likely influenced by interactions with other lung microbiota or their products. The bacterial fermentation product 2,3-butanediol enhances virulence and biofilm formation of *P. aeruginosa* *in vitro*. This study assessed the effects of 2,3-butanediol on *P. aeruginosa* persistence, inflammatory response, and the lung microbiome *in vivo*. Here, *P. aeruginosa* grown in the presence of 2,3-butanediol and encapsulated in agar beads persisted longer in the murine respiratory tract, induced enhanced TNF- $\alpha$  and IL-6 responses and resulted in increased colonization in the lung tissue by environmental microbes. These results led to the following hypothesis that now needs to be tested with a larger study: fermentation products from the lung microbiota not only have a role in *P. aeruginosa* virulence and abundance, but also on the increased colonization of the respiratory tract with environmental microbes, resulting in dynamic shifts in microbiota diversity and disease susceptibility.

The ISME Journal (2016) 10, 2978–2983; doi:10.1038/ismej.2016.76; published online 13 May 2016

Airway microbiome dynamics and microbe-to-microbe interactions are increasingly recognized as critical factors in lung diseases (Cui *et al.*, 2014). Particularly for chronic lung diseases with frequent bacterial infections, such as cystic fibrosis (CF) and chronic obstructive pulmonary disease, airway microbiome dynamics have been associated with disease progression (Hunter *et al.*, 2012, Pragman *et al.*, 2012; Huang *et al.*, 2014). CF predisposes the respiratory tract to polymicrobial infections, and the frequent emergence of *Pseudomonas aeruginosa* is associated with a reduction in bacterial richness (Lynch and Bruce, 2013; Chmiel *et al.*, 2014). Phenotype and virulence of *P. aeruginosa* are affected by interactions with the host and cohabiting microbes (Sibley *et al.*, 2008a; Hunter *et al.*, 2012; Venkataraman *et al.*, 2014; Whiteson *et al.*, 2014). An improved characterization of the human lung microbiome will be instrumental to delineate these interactions (Dickson and Huffnagle, 2015; Venkataraman *et al.*, 2015).

It has been previously demonstrated *in vitro* that the fermentation product 2,3-butanediol, which can be produced by fermenting bacteria, mediates cross-feeding to *P. aeruginosa* and increases biofilm formation and other critical factors of *P. aeruginosa* virulence (Venkataraman *et al.*, 2014). The relevance of this finding was further emphasized by the identification of 2,3-butanedione, which is a volatile compound produced in the same acetoin fermentation pathway as 2,3-butanediol, in the breaths of individuals with CF (Whiteson *et al.*, 2014). 2,3-Butanedione is primarily produced by *Streptococcus* spp. and other fermenters that can potentially cross-feed and enhance *P. aeruginosa* pathogenicity. Here, we evaluate whether 2,3-butanediol increases *P. aeruginosa* virulence within the respiratory tract *in vivo* and assess its effect on the airway microbiota in an agar bead *P. aeruginosa* murine model (Kukavica-Ibrulj and Levesque, 2008). Although the agar bead model of *P. aeruginosa* infection is often used to mimic more chronic infections, as a preliminary study, we investigated the initial acute stage of infection.

*P. aeruginosa* strain PA14 was cultured and encapsulated in agar beads in AB minimal media containing 30 mM of 2,3-butanediol or glucose and then administered to C57Bl/6 mice via the intratracheal route. Controls included empty media agar beads prepared under both conditions. Mice infected

Correspondence: S Worgall, Department of Pediatrics, Weill Cornell Medicine, 505 East 70 Street, Box 211, New York 10021, USA.

E-mail: stw2006@med.cornell.edu

<sup>4</sup>These authors contributed equally to this work.

Received 4 June 2015; revised 31 March 2016; accepted 4 April 2016; published online 13 May 2016

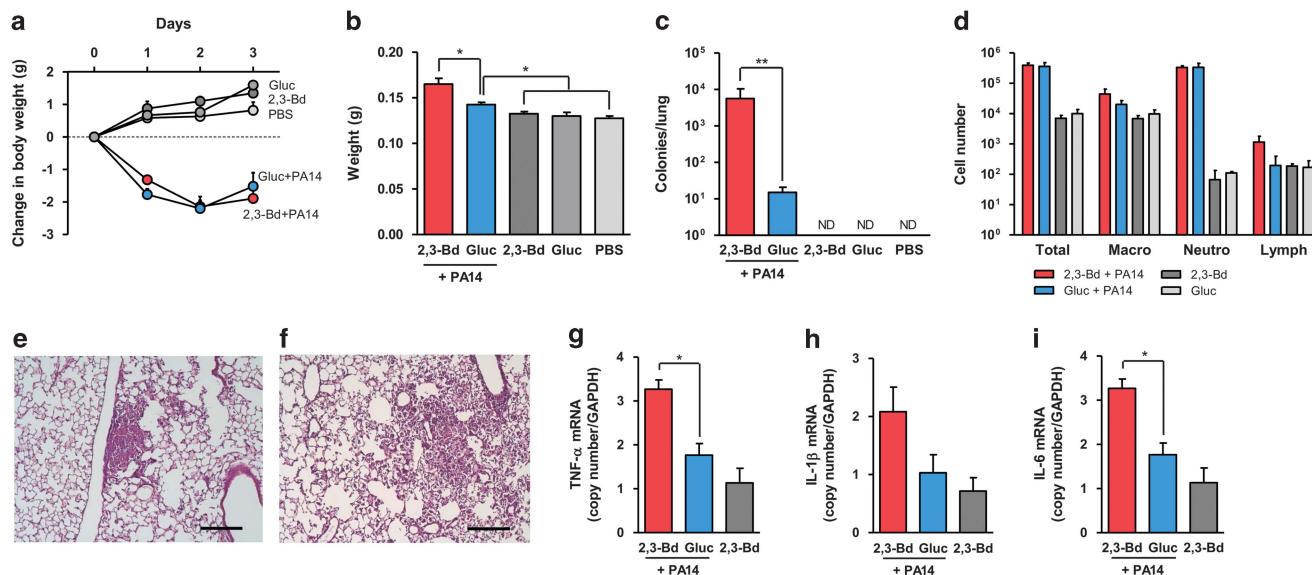


**Figure 1** 2,3-butanediol enhances virulence and persistence of *P. aeruginosa* in the respiratory tract. C57BL/6 mice were infected with agar-encapsulated PA14 grown in the presence of 2,3-butanediol or glucose or with beads with just these substrates. (a) Body weight following infection. (b) Lung weight. (c) *P. aeruginosa* counts from lung homogenates plated on MacConkey agar plates. (d) Bronchioalveolar lavage cellular composition. (e–f) HE-stained lung section two days following PA14 grown in 2,3-butanediol (e) and glucose (f); bar = 200  $\mu$ m. (g–i) Inflammatory cytokine expression in lung. Expression of mRNA of TNF- $\alpha$  (g), IL-1 $\beta$  (h), and IL-6 (i) was quantified by TaqMan Real-Time RT-PCR and normalized to GAPDH RNA. Data are shown as means  $\pm$  s.e.m. of five mice per group. ND = none detected. \* $P$ <0.05; \*\* $P$ <0.001.

with PA14 lost body weight, irrespective of *P. aeruginosa* was grown with 2,3-butanediol or glucose (Figure 1a). Lung weight was increased in both groups that received PA14, indicating considerable inflammation, and was higher with 2,3-butanediol-grown *P. aeruginosa* compared with glucose-grown *P. aeruginosa* (Figure 1b). Clearance of *P. aeruginosa* was delayed in mice infected with PA14 grown in 2,3-butanediol compared with PA14 grown in glucose, as indicated by *P. aeruginosa* quantification after 3 days (Figure 1c). The cellular composition of bronchioalveolar lavage fluid (BAL) showed an increase in neutrophils in mice infected with PA14 grown in 2,3-butanediol and PA14 grown in glucose compared with mice that received beads with only 2,3-butanediol or glucose (Figure 1d). Lung histology showed similar levels of local inflammation in mice infected with PA14 grown in 2,3-butanediol (Figure 1e) and PA14 grown in glucose (Figure 1f). There was, however, an increase in inflammatory cytokines expression in mice infected with PA14 grown in 2,3-butanediol at 3 days of infection (Figures 1g–i). These cytokines are involved in the *P. aeruginosa* lung pathogenesis (Meduri *et al.*, 1999) and lung levels usually peak within the first 24 h following infection with planktonic *P. aeruginosa* (van Heeckeren *et al.*, 2006), while a sustained response that lasts for a few days is present using the agar beads model (van Heeckeren and Schluchter, 2002). Glucose, which was used in our controls, has been shown to inhibit the type III secretion system in *P. aeruginosa*, particularly the secretion of exoS (Rietsch and Mekalanos, 2006). However, strain PA14 does not encode for exoS

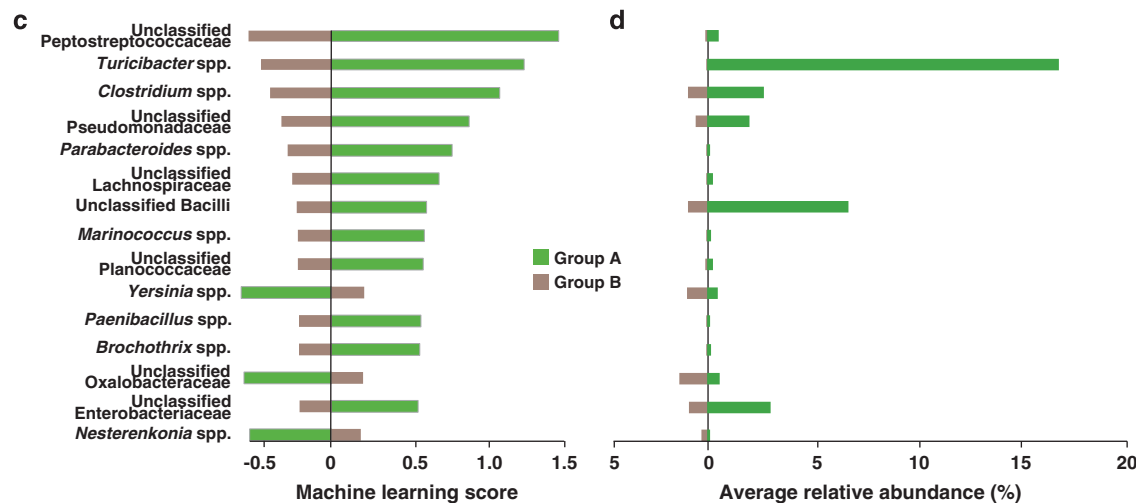
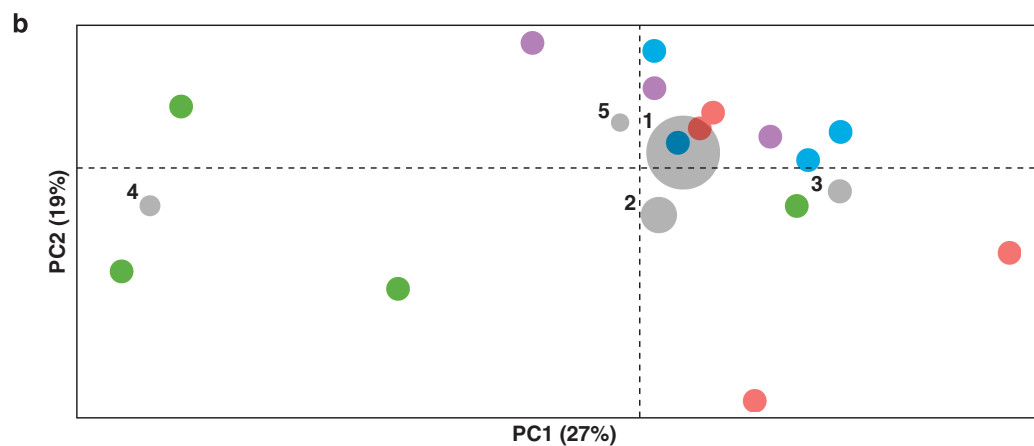
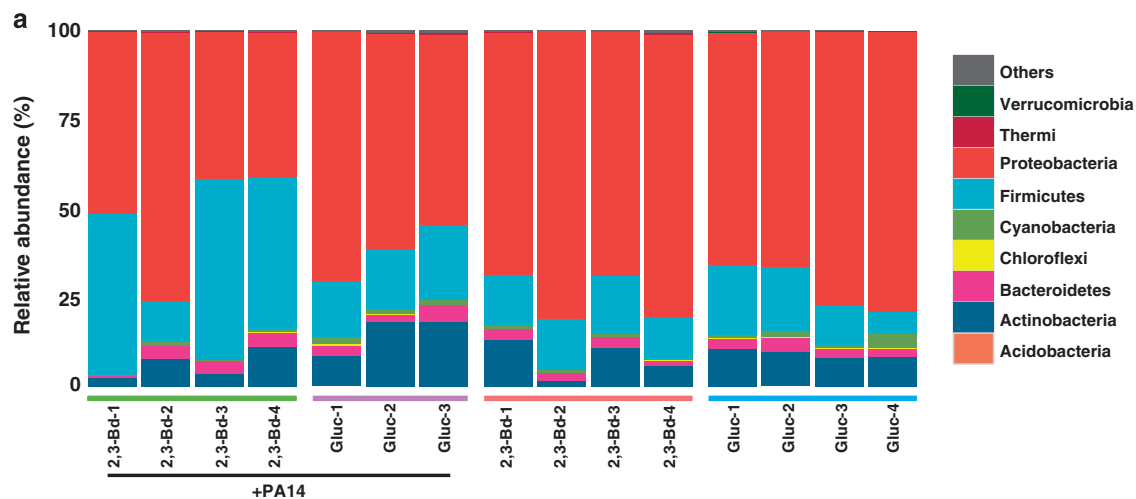
(Miyata *et al.*, 2003) and it is, therefore, unlikely that this mechanism is present here. Furthermore, inhibition of type III secretion system does not affect the replication and survival of *P. aeruginosa* in the lungs of mice (Vance *et al.*, 2005). This strongly suggests that increased virulence of *P. aeruginosa* cultured with 2,3-butanediol, which was previously seen *in vitro* (Venkataraman *et al.*, 2014), translates to increased virulence in the respiratory tract *in vivo*. Compared with conditions in the CF lung, where it is expected that 2,3-butanediol is continuously supplied by co-localized fermenting bacteria, our bead model is limited by the likely decreasing concentrations of 2,3-butanediol by diffusion out of the beads and consumption by *P. aeruginosa*. This could be reflected by the small but significant differences in the acute inflammatory cytokine levels after three days (Figures 1g–i) despite larger differences in the bacterial loads (Figure 1c) between the 2,3-butanediol-exposed lungs and their controls.

After comparing the basal microbiome from lungs (Supplementary Figure S1A) and BAL (Supplementary Figure S1B), Proteobacteria, Firmicutes, Cyanobacteria, Bacteroidetes and Actinobacteria were detected as the most prominent phyla, with similar contributions in lung tissue and BAL for most phyla. Proteobacteria was more abundant in lung tissue samples (37–79%;  $P$ =0.022), while Firmicutes was more abundant in BAL samples (30–39%;  $P$ =0.001). In general, the relative distribution of phyla within each sample was found to be similar to the human respiratory microbiomes from oropharyngeal or BAL samples (Hilty *et al.*, 2010; Erb-Downward *et al.*, 2011; Sze *et al.*, 2012). For

the rest of the study, we selected lung tissue to include all community members within the respiratory tract.

To characterize the murine lung bacterial community, we amplified and sequenced the V4 region of the 16S *rRNA* genes from murine lungs, and observed a total of 3174 unique operational taxonomic units from 924 182 quality sequences (see detailed descriptions of the methods in the

Supplementary Materials). Taxonomic distributions at the phyla level were summarized for each murine lung tissue sample (Figure 2a). The phylum Firmicutes was more abundant ( $P=0.001$ ) in mice that received PA14 in 2,3-butanediol, whereas the relative abundance of Proteobacteria was lower ( $P=0.015$ ). Correlation analysis of sequence and operational taxonomic unit counts per lung tissue showed adequate representation of microbiota



diversity in lung samples irrespective of sample sequence depth (Supplementary Figure S1C). Principal Coordinates Analysis was used to visualize dissimilarities between lung microbiomes. Calculation of weighted UniFrac distances based on taxonomic abundances in each sample showed clustering of lung microbiomes except those treated with PA14 in 2,3-butanediol (Figure 2b), suggesting that lung microbiomes become dissimilar when treated with PA14 in 2,3-butanediol. Analysis with unweighted UniFrac distances showed a similar clustering with less distinction (Supplementary Figure S2). Qualitative visualization of the five most abundant taxa that are driving the dissimilarity between samples indicated that *Turicibacter* spp. contributed to the dissimilarity found in two of four mice lungs treated with PA14 in 2,3-butanediol (Figure 2b, Supplementary figure S2). Supervised machine-learning analysis was performed to quantitatively identify taxa that explain the dissimilarities found in lungs treated with PA14 in 2,3-butanediol (Figure 2c). Caution is needed for such a machine-learning analysis because it is used to generate hypotheses on small data sets that are then validated on larger data sets. Here, we built hypothesis based on a small data set. Lung bacterial communities were classified as Group A (2,3-butanediol with PA14) or Group B (glucose medium with PA14, 2,3-butanediol medium, and glucose medium) and tested with the nearest shrunken centroid method (Tibshirani *et al.*, 2002). This method had already been utilized for supervised learning with microbiota (Knights *et al.*, 2011; Werner *et al.*, 2012) and calculates a machine-learning (prediction) score for each taxon, with a more negative or more positive score indicating better predictability for the taxon. All 593 taxa were ranked for predicting treatment type. The overall machine-learning error rate was 0.19, which indicates that this trained algorithm has an 81% accuracy to classify a murine lung microbiome to its correct treatment type. Although murine lungs that received PA14 in 2,3-butanediol were not significantly more or less diverse than other lungs in our small data set (Supplementary Figures S1D and E), several taxa were found to be closely associated in these lungs, including unclassified genera from the families Peptostreptococcaceae and

Pseudomonadaceae, and the gastrointestinal tract- and feces-associated *Turicibacter* spp., *Clostridium* spp. and *Parabacteroides* spp. (Figures 2c and d). We observed significant increases in the relative taxonomic abundances for the three most predictive taxa from the machine-learning analysis for Group A when compared to Group B (Peptostreptococcaceae  $P=0.001$ ; *Turicibacter* spp.  $P=0.011$ ; *Clostridium* spp.  $P=0.019$ ; Supplementary Figure S3A). A possible source of *Turicibacter* spp. is via coprophagy within the cage, and the same is true for Peptostreptococcaceae and *Clostridium* spp., which are also found in the lower gastrointestinal tract. From these results, we hypothesize that fermentation product 2,3-butanediol from the lung microbiota not only have a role in *P. aeruginosa* virulence and abundance, but also on the increased colonization of the respiratory tract with environmental microbes. In addition, inflammation in the lung may also result in an advantageous environment for *Turicibacter* spp. (Rausch *et al.*, 2015).

To further explore the role of *Pseudomonas* spp. in infection, we compared their relative abundance in the lungs with sample origin and with change in body weight (Supplementary Figure S3D). The colonization of the lungs by environmental microbes (for example, *Turicibacter* spp.), resulted in a decreased relative abundance of *Pseudomonas* spp. In other words, a relative increase in environmental operational taxonomic units for sample 2,3-Bd-3 (Supplementary Figure S3A) caused a relative decrease in *Pseudomonas* spp., but this does not inform the absolute numbers of *P. aeruginosa* (Supplementary Figure S3B). In fact, the corresponding absolute abundance of *P. aeruginosa* was still higher in murine lungs treated with PA14 in 2,3-butanediol even with the increased colonization of environmental microbes (Supplementary Figure S3C). Our results are also consistent with the recent studies that have shown the impact of gut microbiome on acquisition of the lung microbiome in CF (Madan, 2016).

Understanding the microbe-to-microbe interactions that stimulate *P. aeruginosa* virulence and aid in creating a niche for *P. aeruginosa* to persist in the respiratory tract could help to develop novel anti-*P. aeruginosa* strategies by impairing the capa-

**Figure 2** Microbiome of the murine lung. (a) Taxonomic summary of lung microbiota. 16S rRNA gene sequences of lung bacterial community of 15 mice 3 days after infection with varying agar beads treatments, indicated by colored bars above the sample ID: PA14 with 2,3-butanediol (2,3-Bd+PA14, green); PA14 with glucose (Gluc+PA14, purple); 2,3-butanediol medium only (2,3-Bd, red); and glucose medium only (Gluc, blue). Each column represents a sample from one mouse. Bacteria are presented at the phyla level. (b) Principal Coordinates Analysis biplot of murine lung microbiomes. Beta diversity Principal Coordinates Analysis of a weighted UniFrac distance matrix from taxonomic composition within these samples. Only the first two axes are shown. Each circle represents one mouse, which is colored by agar beads treatment: PA14 with 2,3-butanediol (green;  $n=4$ ); PA14 with glucose (purple;  $n=3$ ); 2,3-butanediol medium only (red;  $n=4$ ); and glucose medium only (blue;  $n=4$ ). Gray circles represent taxa coordinates that are calculated based on mean relative abundance (size of circle) for each taxon in all 15 lung samples (1-*Pseudomonas* spp.; 2-*Acinetobacter* spp.; 3-*Escherichia* spp.; 4-*Turicibacter* spp.; 5-*Staphylococcus* spp.). The percentage of distribution described by each axis is as indicated. (c) Machine-learning analysis of murine lung microbiomes. Machine-learning analysis of lung samples binned into two groups based on agar treatment: Group A (2,3-butanediol with PA14; green;  $n=4$ ) and Group B (glucose medium with PA14, 2,3-butanediol medium, and glucose medium; brown;  $n=11$ ). Shown are the 15 highest correlated taxa (of the 593 taxa used to train the algorithm); the overall machine-learning error rate was 0.19 via nearest shrunken centroid method. (d). The average relative abundances of the 15 most predictive taxa from machine-learning analysis, and colored as in c.

city of the lung microbiota to produce fermentation products that we have shown to induce virulence in *P. aeruginosa*. This has been suggested previously by clinical observations that elimination of *Streptococcus milleri*, which is a member of the CF lung microbiota associated with severe exacerbations, led to decreased *P. aeruginosa* virulence (Sibley *et al.*, 2008b). Despite the relatively low microbial densities present in healthy lungs (Dickson and Huffnagle, 2015), alteration of the pulmonary microenvironment to favor a microbial community that is easier to clear may be a promising approach against pulmonary pathogens, which warrant further investigations. A future study with a larger data set to test the hypothesis that was proposed here could help to better understand the role of microbe-to-microbe interactions in disease pathogenesis. Further studies should also include CFTR mutants, ENaC overexpressing mice, later time points, and addition of antibiotics.

## Conflict of Interest

The authors declare no conflict of interest.

## Acknowledgements

This study was supported by a Cornell University Seed Grant for Collaborations between Cornell University-Ithaca and Weill Cornell Medical College Faculty to LTA and SW and a grant from the Sloan Foundation with grant no. 2012-6-04 to LTA. We thank Dr. Kirk Harris (University of Colorado Denver—Anschutz Medical Campus) for fruitful discussions, Catherine Spirito (Cornell University) for microbiome advice, Nancy and Dan Paduano for their enthusiastic support, and anonymous reviewers for suggestions that improved the language of the manuscript.

## References

Chmiel JF, Aksamit TR, Chotirmall SH, Dasenbrook EC, Elborn JS, LiPuma JJ *et al.* (2014). Antibiotic management of lung infections in cystic fibrosis. I. the microbiome, methicillin-resistant staphylococcus aureus, gram-negative bacteria, and multiple infections. *Ann Am Thorac Soc* **11**: 1120–1129.

Cui L, Morris A, Huang L, Beck JM, Twigg HL 3rd, von Mutius E *et al.* (2014). The microbiome and the lung. *Ann Am Thorac Soc* **11**: S227–S232.

Dickson RP, Huffnagle GB. (2015). The lung microbiome: new principles for respiratory bacteriology in health and disease. *PLoS Pathog* **11**: e1004923.

Erb-Downward JR, Thompson DL, Han MK, Freeman CM, McCloskey L, Schmidt LA *et al.* (2011). Analysis of the lung microbiome in the "healthy" smoker and in COPD. *PLoS One* **6**: e16384.

Hilty M, Burke C, Pedro H, Cardenas P, Bush A, Bossley C *et al.* (2010). Disordered microbial communities in asthmatic airways. *PLoS One* **5**: e8578.

Huang YJ, Sethi S, Murphy T, Nariya S, Boushey HA, Lynch SV. (2014). Airway microbiome dynamics

in exacerbations of chronic obstructive pulmonary disease. *J Clin Microbiol* **52**: 2813–2823.

Hunter RC, Klepac-Ceraj V, Lorenzi MM, Grotzinger H, Martin TR, Newman DK. (2012). Phenazine content in the cystic fibrosis respiratory tract negatively correlates with lung function and microbial complexity. *Am J Respir Cell Mol Biol* **47**: 738–745.

Knights D, Costello EK, Knight R. (2011). Supervised classification of human microbiota. *FEMS Microbiol Rev* **35**: 343–359.

Kukavica-Ibrulj I, Levesque RC. (2008). Animal models of chronic lung infection with *Pseudomonas aeruginosa*: useful tools for cystic fibrosis studies. *Lab Anim* **42**: 389–412.

Lynch SV, Bruce KD. (2013). The cystic fibrosis airway microbiome. *Cold Spring Harb Perspect Med* **3**: a009738.

Madan JC. (2016). Neonatal Gastrointestinal and Respiratory Microbiome in Cystic Fibrosis: Potential Interactions and Implications for Systemic Health. *Clin Ther* **38**: 740–746.

Meduri GU, Kanangat S, Stefan J, Tolley E, Schaberg D. (1999). Cytokines IL-1beta, IL-6, and TNF-alpha enhance in vitro growth of bacteria. *Am J Respir Crit Care Med* **160**: 961–967.

Miyata S, Casey M, Frank DW, Ausubel FM, Drenkard E. (2003). Use of the *Galleria mellonella* caterpillar as a model host to study the role of the type III secretion system in *Pseudomonas aeruginosa* pathogenesis. *Infect Immun* **71**: 2404–2413.

Pragman AA, Kim HB, Reilly CS, Wendt C, Isaacson RE. (2012). The lung microbiome in moderate and severe chronic obstructive pulmonary disease. *PLoS one* **7**: e47305.

Rausch P, Steck N, Suwandi A, Seidel JA, Kunzel S, Bhullar K *et al.* (2015). Expression of the Blood-Group-Related Gene B4galnt2 Alters Susceptibility to Salmonella Infection. *PLoS pathogens* **11**: e1005008.

Rietsch A, Mekalanos JJ. (2006). Metabolic regulation of type III secretion gene expression in *Pseudomonas aeruginosa*. *Mol Microbiol* **59**: 807–820.

Sibley CD, Duan K, Fischer C, Parkins MD, Storey DG, Rabin HR *et al.* (2008a). Discerning the complexity of community interactions using a *Drosophila* model of polymicrobial infections. *PLoS pathogens* **4**: e1000184.

Sibley CD, Parkins MD, Rabin HR, Duan K, Norgaard JC, Surette MG. (2008b). A polymicrobial perspective of pulmonary infections exposes an enigmatic pathogen in cystic fibrosis patients. *Proc Natl Acad Sci USA* **105**: 15070–15075.

Sze MA, Dimitriu PA, Hayashi S, Elliott WM, McDonough JE, Gosselink JV *et al.* (2012). The lung tissue microbiome in chronic obstructive pulmonary disease. *Am J Respir Crit Care Med* **185**: 1073–1080.

Tibshirani R, Hastie T, Narasimhan B, Chu G. (2002). Diagnosis of multiple cancer types by shrunken centroids of gene expression. *Proc Natl Acad Sci USA* **99**: 6567–6572.

van Heeckeren AM, Schluchter MD. (2002). Murine models of chronic *Pseudomonas aeruginosa* lung infection. *Lab Anim* **36**: 291–312.

van Heeckeren AM, Schluchter MD, Xue W, Davis PB. (2006). Response to acute lung infection with mucoid *Pseudomonas aeruginosa* in cystic fibrosis mice. *Am J Respir Crit Care Med* **173**: 288–296.

- Vance RE, Rietsch A, Mekalanos JJ. (2005). Role of the type III secreted exoenzymes S, T, and Y in systemic spread of *Pseudomonas aeruginosa* PAO1 *in vivo*. *Infect Immun* **73**: 1706–1713.
- Venkataraman A, Bassis CM, Beck JM, Young VB, Curtis JL, Huffnagle GB *et al.* (2015). Application of a neutral community model to assess structuring of the human lung microbiome. *mBio* **6**: e02284-14.
- Venkataraman A, Rosenbaum MA, Werner JJ, Winans SC, Angenent LT. (2014). Metabolite transfer with the fermentation product 2,3-butanediol enhances virulence by *Pseudomonas aeruginosa*. *ISME J* **8**: 1210–1220.
- Werner JJ, Koren O, Hugenholtz P, DeSantis TZ, Walters WA, Caporaso JG *et al.* (2012). Impact of training sets on classification of high-throughput bacterial 16 s rRNA gene surveys. *ISME J* **6**: 94–103.
- Whiteson KL, Meinardi S, Lim YW, Schmieder R, Maughan H, Quinn R *et al.* (2014). Breath gas metabolites and bacterial metagenomes from cystic fibrosis airways indicate active pH neutral 2,3-butanediol fermentation. *ISME J* **8**: 1247–1258.

Supplementary Information accompanies this paper on The ISME Journal website (<http://www.nature.com/ismej>)